First Storage and Cooling of Secondary Heavy-Ion Beams at Relativistic Energies

H. Geissel, K. Beckert, F. Bosch, H. Eickhoff, B. Franczak, B. Franzke, M. Jung, O. Klepper, R. Moshammer, G. Münzenberg, F. Nickel, F. Nolden, U. Schaaf, C. Scheidenberger, P. Spädtke, M. Steck, and K. Sümmerer

Gesellschaft für Schwerionenforschung, D-61 Darmstadt, Germany

A. Magel

II. Physikalisches Institut der Universität Giessen, D-63 Giessen, Germany

(Received 23 March 1992)

Secondary beams of radioactive heavy ions have been stored and cooled in a storage ring for the first time. Relativistic beams of bare ^{19}Ne and ^{18}F ions were produced by fragmentation of 310 MeV/nucleon ^{20}Ne at the heavy-ion synchrotron at GSI. They were separated in flight with the high-resolution forward spectrometer and injected into the storage-cooler ring. The feasibilities of in-flight lifetime and direct mass measurements for radioactive beams are demonstrated.

PACS numbers: 29.20.Dh, 21.10.−k, 25.75.+r, 29.27.Eg

Recently considerable progress has been made in the production and isotropic separation of secondary beams of exotic nuclei which are created by fragmentation of heavy ions in peripheral collisions [1–3]. The first experiments using relativistic secondary beams have demonstrated new possibilities for studying nuclear structure [4]. Another frontier has been opened with the advent of storage-cooler rings for heavy ions [5]. Both new experimental features are incorporated in the high-energy accelerator complex at GSI. The system consists of the synchrotron SIS [6] providing ions of all elements up to uranium with energies of up to 2 GeV/nucleon, and the experimental storage ring ESR [7] equipped with an electron-cooler facility [8]. Heavy-ion beams up to bismuth have been stored and cooled in the ESR. The cooled beams were characterized by a relative momentum spread of $\Delta p/p < 10^{-5}$ and by a transverse emittance of $\varepsilon < 0.1\pi$ mm mrad [9]. The high-resolution forward spectrometer FRS [10] interconnects the synchrotron and the storage ring (see Fig. 1). It was demonstrated that the FRS efficiently separates isotopically pure fragment beams up to the heaviest projectiles extracted from the SIS.

In the two pilot experiments presented here, the FRS and the ESR were combined for the first time. Secondary beams produced and separated with the FRS were injected and accumulated in the ESR. The experiments aimed at exploring two fields of research: (i) Production and accumulation of bare short-lived β-unstable ions, followed by in-flight determination of their lifetime. This type of experiment was explored with ^{19}Ne ions (half-life: $T_{1/2}=17$ s) as an example. (ii) Production, accumulation, and cooling of both stable and radioactive bare nuclei, followed by a precise direct mass measurement of the circulating beam. Fully ionized ^{18}F ions ($T_{1/2}=1.8$ h) were selected to demonstrate that the ESR can serve as a high-resolution spectrometer for direct mass measurements of secondary beams.

In our experiments a 310 MeV/nucleon $^{20}Ne^{10+}$ beam was extracted from the SIS with a pulse length of about 1 s and focused onto a 4 g/cm^2 beryllium target placed at the entrance of the FRS (Fig. 1). In one SIS cycle about 2×10^9 neon particles were extracted. As a result of reaction kinematics and the slowing-down processes in the production target, the selected fragments had a mean en-

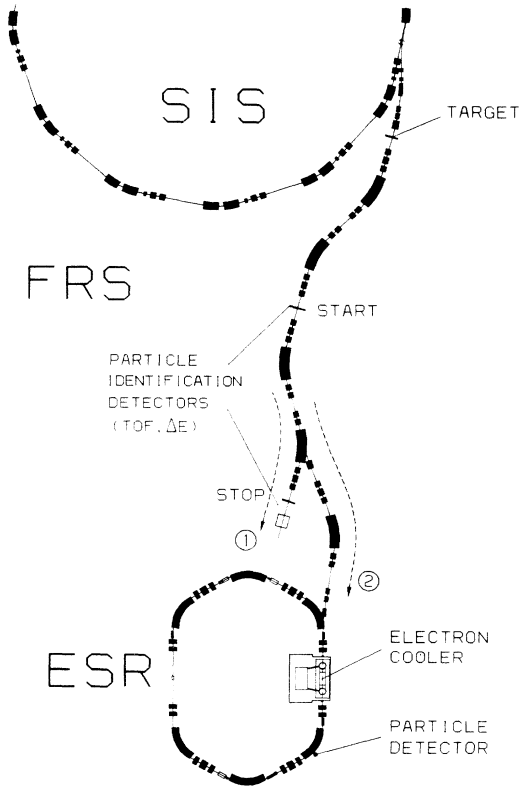

FIG. 1. Layout of the new high-energy facilities at GSI. Using slowly extracted beams from SIS, secondary beams can be separated and identified at the FRS following the flight path marked with 1. For injection into the ESR, the alternate flight path 2 is followed using fast extracted beams from SIS.

ergy of 250 MeV/nucleon and a relative momentum spread (1σ width) of 1% resulting in a transmission through the FRS of about 70%. In this experiment the FRS was used to separate the nuclear reaction products according to their magnetic rigidity ($B\rho$). Since all fragments had approximately the same velocity as the projectile, all nuclei with equal mass-to-charge ratio were separated simultaneously. At this energy the probability for electron capture in the production target is only 10^{-6} [11] allowing an unambiguous $B\rho$ analysis without suffering from ambiguities due to different atomic charge states of the selected reaction products. The separated nuclei were identified with particle detectors at the FRS; see Fig. 1 using the flight path marked with 1. Two position-sensitive scintillators were placed in the central focal plane of the separator (start) and at its exit (stop) to measure the time of flight and the magnetic rigidity of each particle [12]. A segmented ionization chamber with four sections was used to determine the nuclear charge. These detectors are routinely used at the FRS for particle identification and to measure the relative abundances of the separated isotopes [13]. After identification of the desired particles the synchrotron was operated in a fast extraction mode [6], i.e., the projectiles were extracted in one cycle within 1 μs. The last dipole stage of the FRS was switched off and the selected fragments were injected into the ESR along the flight path marked with 2 in Fig. 1 and stored in the injection orbit. More details about this procedure and the available beam diagnostics are given in Ref. [14].

Our first experiment was aimed at production, separation, and storage of a fully ionized ^{19}Ne beam in the ESR and measurement of its in-flight β decay. About 1% of the incident primary beam was converted into ^{19}Ne in the production target. With the fragment separator tuned for ^{19}Ne, all other reaction products with a mass-to-charge ratio of 1.9 were simultaneously injected into the ESR. The main contaminant was ^{15}O with an abundance of 11% with respect to the selected ^{19}Ne. The β^+ decay of a circulating $^{19}Ne^{10+}$ ion into $^{19}F^{9+}$ changes the magnetic rigidity by 10%, which consequently changes its trajectory in the dispersive section of the storage ring. The $^{19}F^{9+}$ ions created in the straight cooler section, i.e., about 16% of all daughter products, were detected with the ESR particle detector [14] shown in Fig. 1. This detector was moved close to the orbit of the circulating ^{19}Ne beam from the direction of higher magnetic rigidity. The β^+ decay pattern shown in Fig. 2 was accumulated during several injection cycles with repetition intervals of 120 s. In this figure the result from a single-component exponential fit is also presented. From the fitted half-life value $\gamma T_{1/2}$ for the laboratory system a half-life of $T_{1/2} = 18.5 \pm 0.6$ s was obtained from the ^{19}Ne rest frame, where γ is the relativistic Lorentz factor ($\gamma = 1.268$ for 250 MeV/nucleon). The value $T_{1/2} = 17.34 \pm 0.09$ s quoted in the literature [15] is consistent with our decay

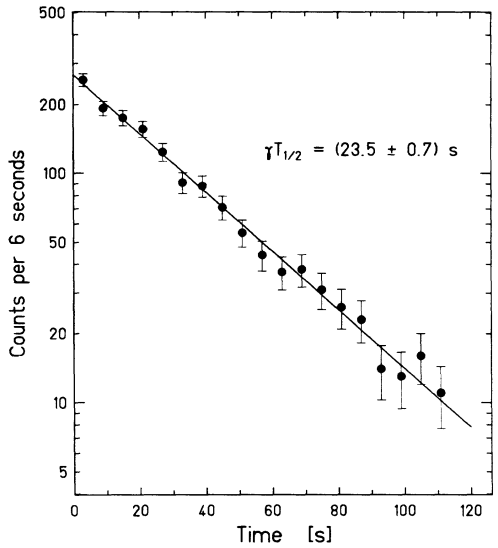

FIG. 2. In-flight β^+ decay of fully ionized 250 MeV/nucleon ^{19}Ne fragments stored in the ESR. The horizontal scale denotes the time after the injection of ^{19}Ne.

pattern due to an 11% ^{15}O contamination with $T_{1/2} = 122$ s. Atomic electron capture of $^{19}Ne^{10+}$ ions in the cooler section, which would be recorded as background in the same detector, can be completely neglected during the short time of data acquisition [9].

The goal of the second part of our experiment was to cool the β-unstable ^{18}F fragments stored in the ESR. About 0.5% of the incident primary beam was converted into ^{18}F in the production target. The selected ^{18}F fragments had a relative momentum spread of 3% resulting in a transmission through the FRS of about 40%. Because of the equal $B\rho$ values the energy-degraded primary beam and the stable nuclei like ^{16}O, ^{14}N, and ^{12}C were injected simultaneously. The masses of ^{20}Ne and ^{14}N were used to determine the mass of the cooled ^{18}F beam (triplet method).

The ESR cooler section has a length of 2 m corresponding to 2% of the ring circumference. The terminal voltage was operated at 137.2 kV. The electron current was 0.5 A corresponding to an electron density of about 8.6×10^6 cm^{-3}. After a cooling time of a few seconds all fragments circulating in the ESR adopted the velocity of the merged electrons. Orbits and revolution frequencies of the stored and cooled fragments are only determined by their mass-to-charge ratios. Capacitive pickups recorded the Schottky noise [16] of the circulating beam. The Schottky spectra, displayed in Fig. 3, were measured at the 49th harmonic of the revolution frequency of the stored and cooled beam. In the upper panel the ^{18}F frequency distribution is clearly resolved in between the corresponding peaks of the stable nuclei of ^{20}Ne and ^{14}N. The intensity ratio of ^{18}F and ^{20}Ne was 0.6×10^{-3} as expected from our measurements using single particle

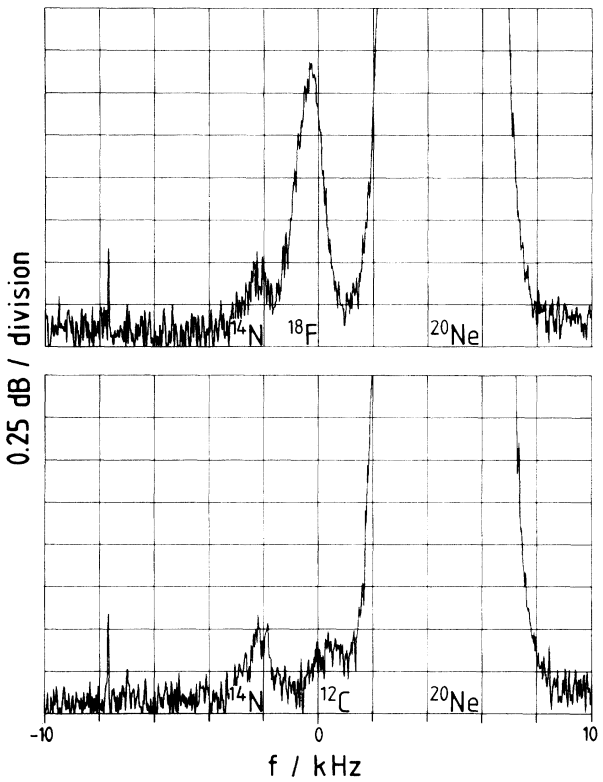

FIG. 3. Schottky spectrum at the 49th harmonic of the revolution frequency of 250 MeV/nucleon ^{18}F fragments measured directly after injection and cooling (top) and 12 h later (bottom). The maximum of the ^{18}F frequency distribution was at 83293 kHz.

identification at the FRS and from the calculated ion-optical transmission. The lower part of the figure shows the Schottky measurement after 12 h without any further injection into the ESR. During the 12 h of storage the electron intensity of the cooler had been reduced to 0.1 A to lower the losses due to atomic radiative electron capture. The signal of the radioactive ^{18}F has practically disappeared during the period of more than six half-lives, whereas the stable isotopes ^{20}Ne and ^{14}N are still observed with only a small loss in intensity. Furthermore, a small additional peak can be observed which was hidden in the tail of the ^{18}F distribution. This peak can be assigned to the frequency distribution of ^{12}C with an intensity less than half of that for ^{14}N which is in agreement with our calculation. The distribution of the stable ^{16}O nuclei could not be resolved in either spectra of Fig. 3 since the difference of the expected centroid and the corresponding one of ^{20}Ne is only 0.68 kHz and the intensity ratio of the two ion species is about 10^{-4}. The influence of contaminants for the determination of the peak maxima was negligible within the quoted uncertainty. In both spectra a very narrow peak was observed 13 kHz below the ^{20}Ne distribution. It can be tentatively assigned to ^{4}He particles.

In the following we will outline the mass determination for the case of $^{18}F^{9+}$. Since the cooling enforces an identical mean velocity upon the circulating ions, the relative separation of two different nuclei in the frequency spectrum $\Delta f_{12}/f_1$, is given by

$$\frac{\Delta f_{12}}{f_1} = -\frac{1}{\gamma_t^2}\frac{\Delta(m/q)_{12}}{(m/q)_1}, \tag{1}$$

where $\gamma_t = 2.70$ is the transition point, a parameter characterizing the ion-optical operating mode of the ESR. In this equation m is the rest mass and q the ionic charge which in our case is equal to the nuclear charge ($q = Z$). The indices 1 and 2 refer to the two nuclides of interest. In our case the selected ratio of A/Z was 2 (A is the mass number); i.e., the separation of the frequency peaks was only determined by the differences in mass defects normalized by the charge states. The relative width (FWHM) $(\Delta f/f)_1$ of the frequency distribution for one selected nuclide is determined by the corresponding velocity spread $(\Delta v/v)_1$,

$$\left(\frac{\Delta f}{f}\right)_1 = \left(\frac{1}{\gamma^2} - \frac{1}{\gamma_t^2}\right)\gamma^2\left(\frac{\Delta v}{v}\right)_1. \tag{2}$$

The masses of two nuclei can be resolved if $\Delta f_{12} \geq \Delta f_1$. The velocity spread (FWHM) of ^{18}F was 1×10^{-5} which corresponds to a mass resolution of 1.9×10^{-5} in the present experiment. However, the mass determination of ^{18}F, the goal of our investigation, can be done more accurately since the distribution is well separated from the selected reference masses of ^{20}Ne and ^{14}N. Therefore the precision of this mass determination is limited by the accuracy of the corresponding peak determinations which in the present experiment corresponds to 60 Hz. The result of our mass measurement for ^{18}F is 17.996008 $\pm$ 0.000085 u. The quoted experimental error corresponds to 80 keV. Our measurement is in excellent agreement with the best value given in the literature [17]: 17.9960034 $\pm$ 0.0000007 u. Since we were dealing with fully ionized ^{18}F particles the literature value was corrected for the mass of the electrons (4599.03 keV) and their total binding energy (2.67 keV). The position of the narrow ^{4}He peak agrees within 1×10^{-4} with the mass value given in Ref. [17]. It is remarkable that the signal for ^{4}He is about 1 order of magnitude narrower compared to that of the other fragments. This could be explained by the reduced influence of intrabeam scattering for low-intensity beams with orbits spatially separated from the high intensity ^{20}Ne beam. Similar observations have been made with heavier ions [18].

Our experiment clearly demonstrates for the first time the high precision of mass determinations for cooled secondary heavy-ion beams. The method becomes even more valuable when applied to nuclei far from stability where the masses are only known with an accuracy of the order of several MeV [19]. The present results demonstrate the pilot character for future experiments with

secondary heavy-ion beams. Two new categories of nuclear physics investigations can be realized: (i) The combination of the storage-cooler ring ESR with the FRS is a powerful tool for measuring the β decay of nuclides in selected ionic charge states. Thus it will be possible to study for the first time in the laboratory nuclear decay properties under conditions similar to those during the stellar nucleosynthesis. (ii) High-resolution nuclear-structure studies are possible with cooled secondary beams. Besides direct mass measurements the high phase-space density also allows precise direct reactions in inverse kinematics, e.g., (p,p'), (d,p) reactions, with the internal gas target of the ESR.

We would like to thank the FRS technicians, the GSI accelerator staff, and the members of the target laboratory for their excellent support, and G. Audi and D. J. Vieira for fruitful discussions.

[1] J. P. Dufour *et al.*, Nucl. Instrum. Methods Phys. Res., Sect. A **248**, 267 (1986).
[2] R. Anne *et al.*, Nucl. Instrum. Methods Phys. Res., Sect. A **257**, 215 (1987).
[3] G. Münzenberg, Nucl. Instrum. Methods Phys. Res., Sect. B (to be published).
[4] I. Tanihata, in *Treatise on Heavy Ion Science*, edited by D. A. Bromley (Plenum, New York, 1989), Vol. 8, p. 443.
[5] D. Habs *et al.*, Nucl. Instrum. Methods Phys. Res., Sect. B **43**, 390 (1989).
[6] K. Blasche *et al.*, Part. Accel. **32**, 83 (1990).
[7] B. Franzke, Nucl. Instrum. Methods Phys. Res., Sect. B **24/25**, 18 (1987); GSI Scientific Report 1991, GSI-92-1 (unpublished).
[8] P. Spädtke *et al.*, in *Proceedings of the Nineteenth INS Symposium on Cooler Rings and Their Applications, Tokyo, Japan, 1990*, edited by T. Katayama and A. Noda (World Scientific, Singapore, 1991), p. 75.
[9] F. Bosch, Nucl. Instrum. Methods (to be published).
[10] H. Geissel *et al.*, Nucl. Instrum. Methods Phys. Res., Sect. B (to be published).
[11] Th. Stöhlker *et al.*, Nucl. Instrum. Methods Phys. Res., Sect. B **61**, 408 (1991).
[12] M. Pfützner *et al.*, GSI Scientific Report 1990, GSI-91-1 (unpublished), p. 288.
[13] K.-H. Schmidt *et al.*, Nucl. Phys. (to be published).
[14] O. Klepper *et al.*, Nucl. Instrum. Methods Phys. Res., Sect. B (to be published).
[15] E. G. Adelberger *et al.*, Phys. Rev. C **27**, 2833 (1983).
[16] U. Schaaf, GSI Report No. 91-22, 1991 (unpublished).
[17] A. H. Wapstra and G. Audi, Nucl. Phys. **A432**, 1 (1985).
[18] B. Franzke (private communication).
[19] P. E. Haustein, At. Data Nucl. Data Tables **39**, 185 (1988).